Journal of Engineering Mathematics (2005) 53: 221–238
DOI 10.1007/s10665-005-5748-z

A spatially nonlocal model for polymer desorption

DAVID A. EDWARDS
Department of Mathematical Sciences, University of Delaware, Newark, DE 19716-2553, USA (E-mail: edwards@math.udel.edu)

Received 20 June 2004; accepted in revised form 21 February 2005

Abstract. In order to describe diffusion of a penetrant in a polymer entanglement network, one must incorporate nonlocal effects. Most previous models have included nonlocality in time only; however, by exploiting the disparate length scales in such systems, one can model these effects by a partial integrodifferential equation which is nonlocal in space. When considering the case of diffusion near the glass-rubber transition, a moving boundary separates the polymer into two regions, each governed by a different set of PDEs. The desorption of a semi-infinite polymer is studied using singular perturbation methods. Layers arise at the exposed surface, at the moving boundary, and initially. Analytical and phase-plane solutions are obtained for the solution, which exhibits physically realistic forms of desorption overshoot. Thus, spatially nonlocal models have the potential to replicate experimental systems, and should be considered in concert with other viscoelastic models of polymer-penetrant systems.

Key words: anomalous diffusion, desorption, moving-boundary-value-problems, polymer-penetrant systems, singular perturbations, spatial nonlocality

1. Introduction

Due to its wide industrial applicability, desorption of penetrants from saturated polymer matrices is of keen interest to experimentalists and scientists. One unusual feature of such systems is the change in the polymer from a *rubbery* state when it is nearly saturated to a *glassy* state when it is nearly dry. As part of the drying process, a glassy region often develops at the exposed surface of a polymer. If this region is dry enough, it can form a *glassy skin* whose properties are significantly different from the rest of the polymer-penetrant solution. One typical system where this occurs is in the desorption of acetone or methanol from poly(methyl-methacrylate), or PMMA [1–4].

This phenomenon, called *literal skinning* [5–7], has many industrial applications. When drying wood, foods, or other agricultural products, the skinning behavior is manifested as "case hardening" [8–10], which can lead to residual stresses that can cause buckling and warping. Skinning behavior has been observed for over a half century in dry spinning and membrane production processes [11, 12]. This glassy skin can be exploited for the production of more effective protective clothing, equipment, or sealants from polymer materials [13, Chapter 17], [14, Chapter 1, Section 4.9], [15]. On the other hand, polymer skinning is undesirable in coating processes due to a decrease in the drying rates and the formation of nonuniformities in the polymer coating [5, 16].

An even more unusual phenomenon, called *trapping skinning*, can also occur. In trapping skinning, an increase in the force driving the desorption will actually *decrease* the accumulated flux through the boundary [3, 11, 17–19]. These various anomalous features of the skinning process cannot be explained by simple Fickian diffusion, which postulates that the chemical potential of the system is a function only of the penetrant concentration $\tilde{C}$.

There are many different theories for why skinning and its associated anomalies occur, including phase separation [20, Section 6], crystallization [21], and diffusion-induced convection [22]. Many scientists believe that one important factor is a nonlocal dependence of the dynamics upon the configuration of the polymer entanglement network. In many polymer-penetrant systems, these nonlocal effects are as important to the transport process as the well-understood Fickian dynamics [23].

Most studies of such nonlocal behavior have focused on viscoelastic memory effects: that is, those that are nonlocal in time only (for instance, see [24–26]). These nonlocal effects in time arise by assuming that the chemical potential is a function not only of $\tilde{C}$, but also of a viscoelastic stress in the polymer [27]. But there are also substantial changes and disparities in length scales in polymer-penetrant systems. These changes must be investigated to see what role they play in the diffusion process.

Polymers form very long chains which can be orders of magnitude larger than the penetrant molecules. The chains intertwine to form an entangement network consisting of a series of interconnected "pockets" through which the penetrant molecules diffuse [28, Chapter 4]. In the rubbery state, the network is disordered, but after the glass transition, the network becomes more highly ordered and even crystalline [29].

Since the intersection of various long polymer chains form these pockets, penetrant diffusion will depend not only on local properties, but also properties within a neighborhood of size β^{-1}, which we shall call the *dependence length*. Thus, we examine the possibility that some of the nonlocal effects are spatial in nature, as in some stochastic models of this type of behavior [30, Chapter 4], [31, p. 288].

We study a model previously presented in [32], where β^{-1} corresponds to the radius of the smallest sphere that contains all the polymer chains forming the walls of a pocket. Clearly β depends on the strength of the entanglement of the polymer network, which is directly related to the amount of penetrant $\tilde{C}$ [28, Chapter 8].

As mentioned above, many models with nonlocal time effects rely on the assumption that the chemical potential does not depend on penetrant alone. In [32], the author adapts this hypothesis by assuming that the chemical potential depends not on $\tilde{C}$ and stress, but on $\tilde{C}$ and a "pseudostress" $\tilde{\sigma}$. This pseudostress depends nonlocally on the spatial distribution of $\tilde{C}$ and its gradient, with β characterizing the decay of the "spatial memory."

In [32], a model is presented which is linear in the gradient of $\tilde{C}$. This then introduces the concept of a "preferred direction", as might be seen in a diffusion-induced convection model [22]. We adapt the model in [32] to enforce a symmetric dependence on the gradient, thus eliminating this artifice.

By choosing such a nonlocal spatial model with symmetric dependence on the gradient, we obtain a partial integrodifferential equation for the penetrant concentration. This can then be restated as a system of two coupled partial differential equations. By making physically appropriate assumptions, the system is reduced to a moving-boundary-value problem (MBVP), where different operators hold on either side of the glass-rubber interface.

We examine the desorption of a semi-infinite saturated polymer film exposed to a drying environment. Figure 1 shows a schematic of the various regions in the problem. Though the glass-rubber interface moves like $\sqrt{\tilde{t}}$, where $\tilde{t}$ is time, the system exhibits several non-Fickian behaviors. Because of the strong dependence of $\tilde{\sigma}$ on $\tilde{C}$, the polymer is dry to leading order in the glassy region; hence the solutions exhibit the unusual phenomenon of *desorption overshoot*, where the minimum in the concentration occurs in the interior of the domain. Such behavior has also been seen in models with nonlocal viscoelastic effects [33].

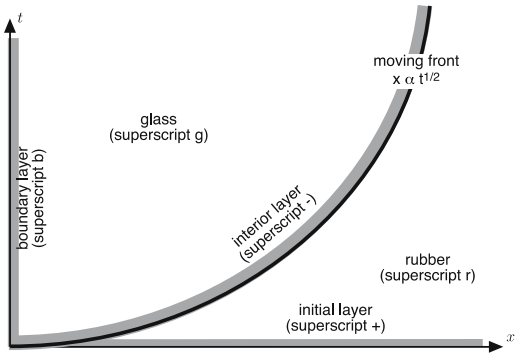

Figure 1. $x-t$ schematic of system.

This behavior causes the problem to be singularly perturbed, and boundary and interior layers are necessary in the glassy region, as shown in Figure 1. Numerical and phase-plane arguments are used to construct the solutions in the layers, while the outer solutions are found analytically. Reasonable conditions on the pseudostress are derived in order to ensure solutions. Some discussion is presented of an initial layer in the system where the full set of equations must hold.

2. Governing equations

As described above, the geometry of the polymer network (especially the pocket structure) implies that the diffusion of penetrant at $(\tilde{x}, \tilde{t})$ will be affected by the material properties of and the dynamics in a neighborhood about the point $(\tilde{x}, \tilde{t})$. To incorporate these effects of polymer entanglement networks into our model, we introduce the following nonstate variable $\tilde{\sigma}$:

$$\tilde{\sigma} = -\frac{1}{2}\int_{-\infty}^{\infty} \left\{ -\eta \tilde{C}(\tilde{x}', \tilde{t}) + \nu \left[\frac{\partial \tilde{C}}{\partial \tilde{x}}(\tilde{x}', \tilde{t}) \right]^2 \right\} \exp\left[-\left| \int_{\tilde{x}'}^{\tilde{x}} \beta(\tilde{C}(z, \tilde{t}))\, \mathrm{d}z \right| \right] \mathrm{d}\tilde{x}', \tag{2.1}$$

where $\eta > 0$ and ν are constants.

As written in (2.1), the exponential part of $\tilde{\sigma}$ models the decaying spatial nonlocality in the polymer network, with a characteristic dependence length β^{-1}. The dynamics of penetrant transport that are "remembered" are encapsulated in the braced term. The form chosen achieves three key goals:

(1) It includes the dynamics of both $\tilde{C}$ and its gradient.
(2) It is symmetric in $\partial \tilde{C}/\partial \tilde{x}$, which is desirable to eliminate a preferred direction, as discussed in Section 1.
(3) Because a quadratic term is used, rather than $|\partial \tilde{C}/\partial \tilde{x}|$, it can be thought of as the first part of a Taylor series for a more complicated function $f(\tilde{C}, \partial \tilde{C}/\partial \tilde{x})$.

Here the sign of η has been chosen so that a positive uniform concentration corresponds to a positive pseudostress. In addition, we expect that the first braced term (which has an analogy to a local swelling term in the viscoelastic case) will dominate the expression, since the gradient terms are second-order effects. This size ordering will become explicit when the equations are scaled.

Note that $\tilde{\sigma}$ satisfies the evolution equation

$$\frac{\partial}{\partial \tilde{x}}\left[\frac{1}{\beta(\tilde{C})}\frac{\partial \tilde{\sigma}}{\partial \tilde{x}}\right]-\beta(\tilde{C})\tilde{\sigma}=-\eta\tilde{C}+\nu\left(\frac{\partial \tilde{C}}{\partial \tilde{x}}\right)^2, \tag{2.2}$$

which is quite similar to the viscoelastic evolution equation in [26] with $\partial/\partial\tilde{t}$ replaced by $\partial^2/\partial\tilde{x}^2$ – in other words, we replace one part of the diffusion operator with another. Physically, one can also think of $\tilde{\sigma}$ as a quantity that diffuses through the polymer. This would necessitate replacing the first term in (2.2) with the complete diffusion operator. But then taking a quasisteady-state approximation of such an equation would result in the form in (2.2).

As discussed in [32] (which can be consulted for further details), we propose that the chemical potential depends not only on $\tilde{C}$, but also on $\tilde{\sigma}$. Thus conservation of mass becomes

$$\frac{\partial \tilde{C}}{\partial \tilde{t}}=\frac{\partial}{\partial \tilde{x}}\left[\tilde{D}(\tilde{C})\frac{\partial \tilde{C}}{\partial \tilde{x}}+\tilde{E}(\tilde{C})\frac{\partial \tilde{\sigma}}{\partial \tilde{x}}\right], \tag{2.3}$$

where $\tilde{E}(\tilde{C})$ is a pseudostress diffusion coefficient and $\tilde{D}(\tilde{C})$ is the molecular diffusion coefficient.

At this stage the reader may ask why β, $\tilde{D}$, and $\tilde{E}$ depend only on $\tilde{C}$, rather than $\tilde{\sigma}$. On a basic level, $\tilde{\sigma}$ depends on $\tilde{C}$, so all the parameters may be written with the simpler functional form. More fundamentally, by making the parameters depend on $\tilde{\sigma}$ directly, we would introduce nonlocal effects into their evolution. For the viscoelastic case it has been shown [34, 35] that introducing nonlocal effects into the parameters does not change the nature of the system. Keeping in mind the parallels between this model and the viscoelastic case, we hence keep the similar functional form shown for our parameters.

Equations (2.2) and (2.3), which form the full nonlinear system we must solve, are complicated enough that it would require a complete numerical solution in order to solve them in general. Unfortunately, such numerical solutions do not easily show the dependence of the solution on the underlying material parameters. Thus we wish to use a singular perturbation approach to derive analytical solutions.

This can be effected by noting that, as described above, the polymer entanglement network can be characterized by two states. When the penetrant concentration is less than some threshold value $\tilde{C}_*$, the polymer is glassy and characterized by well-ordered, severely entangled polymer chains. If $\tilde{C}>\tilde{C}_*$, the polymer is rubbery, the network disentangles, and the characteristic length of a chain grows [23, 29]. Hence $\beta(\tilde{C})$ increases greatly as the polymer goes from the glassy to the rubbery state. Since the differences in $\beta(\tilde{C})$ *within* states are less important than differences *between* states, we model $\beta(\tilde{C})$ by its average in each phase, yielding the following functional form:

$$\beta(\tilde{C})=\begin{cases}\beta_{\mathrm{g}}, & 0\le\tilde{C}\le\tilde{C}_*\\ \beta_{\mathrm{r}}, & \tilde{C}_*<\tilde{C}\le\tilde{C}_{\mathrm{c}},\end{cases}\qquad \beta_{\mathrm{r}}\gg\beta_{\mathrm{g}}, \tag{2.4}$$

where sub- and superscripts "g" refer to the glassy region and sub- and superscripts "r" refer to the rubbery region. $\tilde{D}$ and $\tilde{E}$ will also be chosen piecewise constant, as described later in this section.

Clearly these piecewise-constant functional forms are a simplification; the true dependence length is a smooth function of $\tilde{C}$. Nevertheless, the use of such a simplified model has a long history of yielding analytically tractable results which match experiment well [12, 36–40]. With these piecewise-constant functional forms, our system becomes an MBVP for the glass-rubber interface $\tilde{s}(\tilde{t})$, which separates the $\tilde{x}$–$\tilde{t}$ plane into glassy and rubbery domains.

Also, a real experimental system will deal with an initially saturated slab of finite thickness. However, if the slab is relatively thick, it may be modeled by the more analytically tractable case of a semi-infinite polymer. Moreover, we choose the concentration in the slab initially to be a uniform value C_c.

To simplify the problem, we introduce dimensionless variables. We scale $\tilde{x}$ by the longer, more experimentally observable glassy length scale, and concentrations by the initial concentration. We scale the pseudostress so that the nonlinear term in (2.2) is $O(1)$, and the time scale to simplify the dimensionless form of $\tilde{E}$. In summary, we have

$$x = \tilde{x}\beta_g, \quad t = \tilde{t}\nu\beta_g^3 C_c \tilde{E}_g, \quad s(t) = \beta_g \tilde{s}(\tilde{t}), \quad C(x,t) = \frac{\tilde{C}(\tilde{x},\tilde{t})}{C_c}, \tag{2.5a}$$

$$\sigma(x,t) = \frac{\tilde{\sigma}(\tilde{x},\tilde{t})}{\nu C_c^2 \beta_g}, \quad D(C) = \frac{\tilde{D}(\tilde{C})}{\nu\beta_g C_c \tilde{E}_g}, \quad E(C) = \frac{\tilde{E}(\tilde{C})}{\tilde{E}_g}, \tag{2.5b}$$

where $\tilde{E}_g$ is the value of $\tilde{E}$ in the glassy region.

We make several additional physically reasonable simplifying assumptions so that the problem is more analytically tractable. As with $\beta(\tilde{C})$, the molecular diffusion coefficient $D(C)$ also increases dramatically as the polymer goes from the glassy to rubbery state [37]. The true increase is continuous; some authors model it with an exponential [21, 41]. However, in order to obtain analytic solutions, we follow the lead of [12, 36–40] and perform the same sort of averaging we use with β to obtain our functional form for $D(C)$:

$$D(C) = \begin{cases} D_g, & 0 \le C \le C_*, \\ D_r, & C > C_*, \end{cases} \qquad D_r > D_g. \tag{2.6}$$

In addition, we use the same technique for the pseudostress coefficient. With the scalings in (2.5), its functional form becomes

$$E(C) = \begin{cases} 1, & 0 \le C < C_*, \\ E_r, & C_* < C \le 1, \end{cases} \qquad E_r > 1. \tag{2.7}$$

As in [32], we take $\beta_r/\beta_g = \epsilon$ to be the small parameter we use in our perturbation approach. Substituting (2.5–2.7) in (2.2) and (2.3), we have the following equations in the glass:

$$\frac{\partial C^g}{\partial t} = D_g \frac{\partial^2 C^g}{\partial x^2} + \frac{\partial^2 \sigma^g}{\partial x^2}, \tag{2.8a}$$

$$\frac{\partial^2 \sigma^g}{\partial x^2} - \sigma^g = -b\epsilon^{-1} C^g + \left(\frac{\partial C^g}{\partial x}\right)^2, \quad b = \frac{\eta\epsilon}{\nu\beta_g^2 C_c}, \tag{2.8b}$$

where the size of b is chosen to emphasize that we expect the C^g term in (2.8b) to dominate. Substituting (2.5–2.7) in (2.2) and (2.3), we obtain the following equations in the rubber:

$$\frac{\partial C^r}{\partial t} = D_r \frac{\partial^2 C^r}{\partial x^2} + E_r \frac{\partial^2 \sigma^r}{\partial x^2}, \tag{2.9a}$$

$$\frac{\partial^2 \sigma^r}{\partial x^2} - \epsilon^{-2}\sigma^r = -b\epsilon^{-2} C^r + \epsilon^{-1}\left(\frac{\partial C^r}{\partial x}\right)^2. \tag{2.9b}$$

Now we postulate appropriate boundary and initial conditions for our problem. As discussed above, we have scaled the concentration by the uniform initial condition. Thus we have

$$C(x,0) = 1. \tag{2.10}$$

At the exposed interface $x=0$, we must apply two conditions. The first is a *radiation condition*: that is, the flux through the inside of the film is proportional to the difference between the concentration at the edge of the film and the exterior concentration C_{ext}. For simplicity, we examine the case of a large mass transfer coefficient k so that the evolution proceeds quickly:

$$D(C)\frac{\partial C}{\partial x}(0,t)+E(C)\frac{\partial \sigma}{\partial x}(0,t)=k\epsilon^{-1/2}[C(0,t)-C_{\text{ext}}]. \tag{2.11a}$$

The choice of the exponent $-1/2$ will be explained in Section 3.

Due to the form of the evolution Equation (2.2), we must impose a second boundary condition on the pseudostress at the exposed edge $x=0$. (This is in contrast to the viscoelastic case, where an initial condition for the stress must be imposed.) Since (2.11a) already provides a conditon on $\partial\sigma/\partial x$, we now impose a Dirichlet conditon on σ:

$$\sigma(0,t)=\sigma_{\text{in}}(t), \tag{2.11b}$$

where the subscript "in" stands for "interface". Note that this boundary condition is generic enough to model various situations which might occur in the lab, and we expect experiments to suggest what the proper form of σ_{in} should be.

Since the MBVP we have created between rubber and glass is a mathematical construct, we must choose what conditions to impose at the moving boundary $s(t)$. Some authors treat the dymanics at $s(t)$ with a kinetic-type condition [21, 38]. However, since the true physical parameters in the problem are all continuous, we impose continuity of the dependent variables at $s(t)$. In particular, the concentration must be continuous at a specified transition value C_*:

$$C^{\text{r}}(s(t),t)=C_*=C^{\text{g}}(s(t),t). \tag{2.12a}$$

The pseudostress must also be continuous, though we do not know its value:

$$\sigma^{\text{r}}(s(t),t)=\sigma^{\text{g}}(s(t),t). \tag{2.12b}$$

Lastly, the flux across the interface must be continuous. Given the fact that (2.12a) holds, this condition becomes the following:

$$\left(D_{\text{r}}\frac{\partial C}{\partial x}+E_{\text{r}}\frac{\partial \sigma}{\partial x}\right)(s^{+}(t),t)=\left(D_{\text{g}}\frac{\partial C}{\partial x}+\frac{\partial \sigma}{\partial x}\right)(s^{-}(t),t). \tag{2.12c}$$

There may be some concern about whether imposing continuity of the dependent variables is consistent with our piecewise-constant choice of parameters. However, since $\partial\sigma/\partial x$ *can* have a discontinuity across the interface (it is only the combined term forming the flux that cannot), (2.2) can be satisfied in an integral sense across the jump at $s(t)$.

In the remaining sections we use perturbation methods to analyze our system as described above. In Section 3 we derive the concentration in the glassy region. Since the outer solution does not match our boundary conditions, layers must be inserted near the boundary $x=0$ and the moving interface $x=s(t)$. In Section 4 we derive the remaining outer solutions and use them to determine the behavior of the moving front $x=s(t)$. Our solutions do not fully satisfy the initial conditions, and so an initial layer must also be inserted. Since such a layer does not appreciably affect the solution, it is discussed in Appendix A.

3. Preliminaries

We now examine the glassy region. We assume a perturbation series for our solutions in ϵ:

$$C^{\mathrm{g}}(x,t;\epsilon)=C_0^{\mathrm{g}}(x,t)+O(\epsilon^{1/2}),\qquad \sigma^{\mathrm{g}}(x,t;\epsilon)=\sigma_0^{\mathrm{g}}(x,t)+O(\epsilon^{1/2}), \tag{3.1}$$

where the size of the error term is motivated by (2.11a). Substituting (3.1) in (2.8), we obtain

$$\frac{\partial C_0^{\mathrm{g}}}{\partial t}=D_{\mathrm{g}}\frac{\partial^2 C_0^{\mathrm{g}}}{\partial x^2}+\frac{\partial^2\sigma_0^{\mathrm{g}}}{\partial x^2}, \tag{3.2a}$$

$$\frac{\partial^2\sigma_0^{\mathrm{g}}}{\partial x^2}-\sigma_0^{\mathrm{g}}=-b\epsilon^{-1}C_0^{\mathrm{g}}+\left(\frac{\partial C_0^{\mathrm{g}}}{\partial x}\right)^2. \tag{3.2b}$$

The leading order of (3.2b) is given by

$$C_0^{\mathrm{g}}\equiv 0, \tag{3.3}$$

and hence we see that a glassy skin has formed where the polymer is dry (to leading order). However, the leading order of (2.11a) becomes

$$C_0^{\mathrm{g}}(0,t)=C_{\mathrm{ext}}. \tag{3.4}$$

Equation (3.4) implies that on the t time scale, the exposed edge is always glassy. Therefore, there must be an initial layer where the polymer quickly transitions from rubber to glass. This high rate of desorption in the rubber has been observed experimentally [38, 42, 43]; more discussion of the initial layer can be found in Appendix A.

3.1. Boundary layer

Since (3.3) does not satisfy (3.4), there must be a boundary layer about $x=0$. Thus we introduce the following boundary-layer scaling:

$$C^{\mathrm{g}}(x,t;\epsilon)=C_0^{\mathrm{b}}(\xi,t)+O(\epsilon^{1/2}),\qquad \sigma^{\mathrm{g}}(x,t;\epsilon)=\sigma_0^{\mathrm{b}}(\xi,t)+O(\epsilon^{1/2}),\qquad \xi=\frac{x}{\epsilon^{1/2}}. \tag{3.5}$$

Substituting (3.5) in (2.8a) and integrating, we see that to leading order ($O(\epsilon^{-1/2})$), the flux must be constant in the interface. But the flux in the outer region is $O(1)$, so we must have that

$$D_{\mathrm{g}}\frac{\partial C_0^{\mathrm{b}}}{\partial\xi}+\frac{\partial\sigma_0^{\mathrm{b}}}{\partial\xi}=0. \tag{3.6a}$$

In addition, substituting (3.5) in (2.11a) yields

$$\left(D_{\mathrm{g}}\frac{\partial C_0^{\mathrm{b}}}{\partial\xi}+\frac{\partial\sigma_0^{\mathrm{b}}}{\partial\xi}\right)(0,t)=k[C_0^{\mathrm{b}}(0,t)-C_{\mathrm{ext}}]. \tag{3.6b}$$

Note that the choice of $\epsilon^{-1/2}$ in (2.11a) forces a dominant balance in (3.6b).

Combining (3.6), we must have that

$$C_0^{\mathrm{b}}(0,t)=C_{\mathrm{ext}}. \tag{3.7a}$$

Upon substituting (3.7a) in (3.6b), we see that to leading order, there is no flux through the interface. This is physically reasonable, because here the leading order is $O(\epsilon^{-1/2})$. Since the

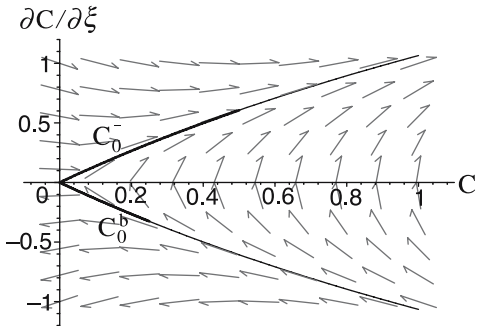

Figure 2. Phase-plane characterizing boundary- and interior-layer solutions. The separatrix is indicated with a thin line; the thick line is the solution indicated.

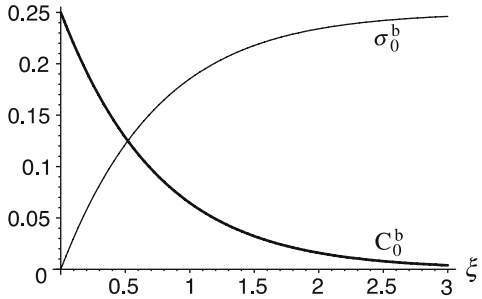

Figure 3. Plot of σ_0^{b} and C_0^{b} in boundary layer.

skin is known to slow desorption [16, 17], it is clear that the flux through the skin should be no larger than $O(1)$. The last condition needed for our layer problem is a matching condition; we note from (3.3) that the appropriate one for our problem is

$$C_0^{\mathrm{b}}(\infty, t) = C_0^{\mathrm{g}}(0, t) = 0. \tag{3.7b}$$

Substituting (3.5) in (2.8b), we obtain, to leading order,

$$\frac{\partial^2 \sigma_0^{\mathrm{b}}}{\partial \xi^2} = -bC_0^{\mathrm{b}} + \left(\frac{\partial C_0^{\mathrm{b}}}{\partial \xi}\right)^2, \tag{3.8a}$$

$$D_{\mathrm{g}} \frac{\partial^2 C_0^{\mathrm{b}}}{\partial \xi^2} - bC_0^{\mathrm{b}} = -\left(\frac{\partial C_0^{\mathrm{b}}}{\partial \xi}\right)^2, \tag{3.8b}$$

where in the second line we have used (3.6a). The second-order ODE (3.8b) may be written as a phase-plane system which has a saddle point at the origin corresponding to the matching condition given by (3.7b). After choosing the following parameters:

$$D_{\mathrm{g}} = 1, \qquad b = 2, \tag{3.9a}$$

we plot the phase plane in Figure 2.

Because the matching condition at $\xi = \infty$ corresponds to the saddle point, the solution we seek is a segment of one of the two stable separatrices. Upon choosing

$$C_{\mathrm{ext}} = 1/4, \tag{3.9b}$$

the portion of the separatrix representing the solution is easily drawn using (3.7a), as indicated in Figure 2. We may also use the rather amazing fact that (3.8b) can be integrated once to yield

$$\frac{\partial C_0^{\mathrm{b}}}{\partial \xi} = -\sqrt{\frac{bD_{\mathrm{g}}}{2}} \left[\frac{2C_0^{\mathrm{b}}}{D_{\mathrm{g}}} - 1 + \exp\left(-\frac{2C_0^{\mathrm{b}}}{D_{\mathrm{g}}}\right)\right]^{1/2}, \tag{3.10}$$

where we have taken the negative square root since C_0^{b} is always decreasing. We may solve (3.10) numerically given the condition (3.7a).

We would also like to compute the pseudostress, which necessitates integrating (3.6a) once more. Thus we need the boundary condition on σ at $\xi = 0$, which is simply given by (2.11b). Integrating (3.6a) using (3.7a) and this constraint, we obtain

$$\sigma_0^{\mathrm{b}}(\xi, t) = D_{\mathrm{g}}(C_{\mathrm{ext}} - C_0^{\mathrm{b}}) + \sigma_{\mathrm{in}}(t). \tag{3.11}$$

Now that we have expressions for both the concentration and σ, we can plot our solutions once we choose our remaining parameters:

$$C_* = 1/2, \quad \sigma_{\mathrm{in}}(t) = 0. \tag{3.12}$$

Figure 3 shows a graph of both C_0^{b} and σ_0^{b} on the same graph for the parameters in (3.9) and (3.12). Here $\xi = 0$ corresponds to the boundary, so we see that $C_0^{\mathrm{b}} = C_*$ and $\sigma_0^{\mathrm{b}} = 0$ there. Thus we have a smooth (but sharp) transition from the values at the exposed interface to the values in the glassy skin. Note that in order for the flux through the interface to remain moderate, the large concentration gradient in the layer between the interface and dry value must be balanced by an equally large and oppposite psuedostress gradient.

3.2. Interior layer

Since (3.3) does not satisfy (2.12a), there must also be an interior layer about $x = s(t)$. Thus we introduce the following interior-layer scaling:

$$\zeta = \frac{x - s(t)}{\epsilon^{1/2}}, \quad C^{\mathrm{g}}(x, t; \epsilon) = C_0^-(\zeta, t) + \epsilon^{1/2} C_1^-(\zeta, t) + o(\epsilon^{1/2}), \tag{3.13a}$$

$$\sigma^{\mathrm{g}}(x, t; \epsilon) = \sigma_0^-(\zeta, t) + \epsilon^{1/2} \sigma_1^-(\zeta, t) + o(\epsilon^{1/2}). \tag{3.13b}$$

Substituting (3.13) in (2.8a) and integrating, we again can use order-of-magnitude arguments to determine that the leading-order flux must be zero at the moving front:

$$D_{\mathrm{g}} \frac{\partial C_0^-}{\partial \zeta} + \frac{\partial \sigma_0^-}{\partial \zeta} = 0. \tag{3.14}$$

Substituting (3.13) in (2.8b), we obtain the following, to leading order:

$$\frac{\partial^2 \sigma_0^-}{\partial \zeta^2} = -b C_0^- + \left(\frac{\partial C_0^-}{\partial \zeta} \right)^2. \tag{3.15}$$

But (3.14) and (3.15) contain the same operators as (3.6a) and (3.8a). The only difference is the fact that (3.7b) is replaced by the new matching condition

$$C_0^-(-\infty, t) = C_0^{\mathrm{g}}(s(t), t) = 0. \tag{3.16}$$

Thus in this case a portion of the unstable separatrix is required.

Note that the boundary $\zeta = 0$ now corresponds to the front $x = s(t)$, so the boundary condition is

$$C_0^-(0, t) = C_*. \tag{3.17}$$

Then using (3.17), we may easily indicate that portion of the separatrix corresponding to our solution, as shown in Figure 2. The parameters are the same as used above.

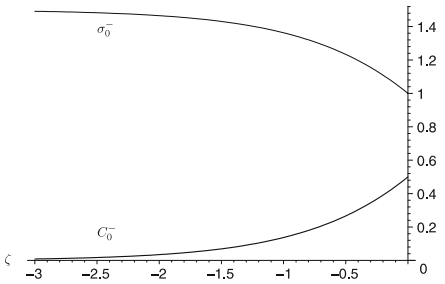

Figure 4. Plot of σ_0^- and C_0^- in interior layer.

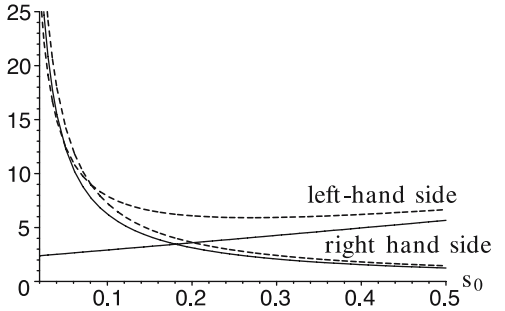

Figure 5. Plot of the expressions in (4.11). Solid lines: $\sigma_{\text{in}} = 0$, $D_{\text{g}} = 1$. Dotted lines: $\sigma_{\text{in}} = 1$, $D_{\text{g}} = 1{\cdot}8$.

Because of the similarities between the operators, (3.10) is replaced by

$$\frac{\partial C_0^-}{\partial \zeta} = \sqrt{\frac{bD_{\text{g}}}{2}} \left[\frac{2C_0^-}{D_{\text{g}}} - 1 + \exp\left(-\frac{2C_0^-}{D_{\text{g}}} \right) \right]^{1/2}, \tag{3.18}$$

where we have taken the positive square root since C_-^0 is always increasing.

We would also like to compute σ, which necessitates integrating (3.14) once more. Since we have already used the condition at $\zeta = -\infty$, we must use the condition at the front $x = s(t)$, which corresponds to $\zeta = 0$. To calculate this value, we examine the pseudostress in the rubbery region. We assume a perturbation series for our rubbery solutions in ϵ:

$$C^{\text{r}}(x, t; \epsilon) = C_0^{\text{r}}(x, t) + O(\epsilon^{1/2}), \qquad \sigma^{\text{r}}(x, t; \epsilon) = \sigma_0^{\text{r}}(x, t) + O(\epsilon^{1/2}). \tag{3.19}$$

Substituting (3.19) in (2.9b), we have the following, to leading order:

$$-\sigma_0^{\text{r}} = -bC_0^{\text{r}}, \tag{3.20}$$

and hence $\sigma_0^-(0, t) = bC_*$. Integrating (3.14) using (3.17) and this fact, we obtain

$$\sigma_0^-(\zeta, t) = D_{\text{g}}(C_* - C_0^-) + bC_*. \tag{3.21}$$

Now that we have expressions for both the concentration and σ, we can plot our solutions, again using the parameters above. Figure 4 shows a graph of both C_0^- and σ_0^- on the same graph for the parameters in (3.9) and (3.12). Here $\zeta = 0$ corresponds to the front, so we see that $C_0^- = C_*$ there. Note there is an internal maximum in the pseudostress associated with the change of state from rubber to glass. This maximum has been seen in other theoretical [44–46] and experimental [47] studies of these types of systems.

4. Computing the solution

4.1. Outer solutions

We now examine the outer solution for σ in the glassy region. Substituting (3.3) in (3.2a) yields

$$\frac{\partial^2 \sigma_0^{\text{g}}}{\partial x^2} = 0. \tag{4.1}$$

The boundary conditions on (4.1) are given by the matching conditions as we exit each of the layers. Solving (4.1) subject to these conditions, we obtain

$$\sigma_0^{\mathrm{g}}(x,t)=\left[D_{\mathrm{g}}C_{\mathrm{ext}}+\sigma_{\mathrm{in}}(t)\right]\left[1-\frac{x}{s(t)}\right]+(D_{\mathrm{g}}+b)C_*\frac{x}{s(t)}. \tag{4.2}$$

In order to complete the coupling of the glassy and rubbery regions, we substitute (3.13) in (2.12c) to obtain, to leading order,

$$\left(D_{\mathrm{g}}\frac{\partial C_1^-}{\partial\zeta}+\frac{\partial\sigma_1^-}{\partial\zeta}\right)(0,t)=(D_{\mathrm{r}}+bE_{\mathrm{r}})\frac{\partial C_0^{\mathrm{r}}}{\partial x}(s(t),t), \tag{4.3}$$

where we have used (3.14) and (3.20). The other condition may be obtained by examining the next order of (2.8a) and the left matching condition in the interior layer:

$$D_{\mathrm{g}}\frac{\partial^2 C_1^-}{\partial\zeta^2}+\frac{\partial^2\sigma_1^-}{\partial\zeta^2}=-\dot{s}\frac{\partial C_0^-}{\partial\zeta}, \tag{4.4a}$$

$$\left(D_{\mathrm{g}}\frac{\partial C_1^-}{\partial\zeta}+\frac{\partial\sigma_1^-}{\partial\zeta}\right)(-\infty,t)=\left(D_{\mathrm{g}}\frac{\partial C_0^{\mathrm{g}}}{\partial x}+\frac{\partial\sigma_0^{\mathrm{g}}}{\partial x}\right)(s(t),t), \tag{4.4b}$$

where the dot indicates differentiation with respect to t. Integrating (4.4a) subject to (4.4b) and then evaluating the result at $\zeta=0$, we have

$$\left(D_{\mathrm{g}}\frac{\partial C_1^-}{\partial\zeta}+\frac{\partial\sigma_1^-}{\partial\zeta}\right)(0,t)-\frac{\partial\sigma_0^{\mathrm{g}}}{\partial x}(s(t),t)=-\dot{s}C_*, \tag{4.5}$$

where we have used (3.3), (3.16), and (3.17). Combining Equations (4.3) and (4.5) using (4.2), we obtain the following:

$$(D_{\mathrm{r}}+bE_{\mathrm{r}})\frac{\partial C_0^{\mathrm{r}}}{\partial x}(s(t),t)=\frac{(D_{\mathrm{g}}C_*+bC_*)-\left[D_{\mathrm{g}}C_{\mathrm{ext}}+\sigma_{\mathrm{in}}(t)\right]}{s}-\dot{s}C_*. \tag{4.6}$$

Equation (4.6) now provides the necessary boundary condition on the rubbery solution to couple the states together. It is quite similar to the interface condition for a one-phase Stefan problem, with a few key differences. The presence of an s in the denominator is unusual, but has been seen in viscoelastic MBVP models of these systems [26]. Also, the sign of the $\dot{s}$ term is negative, while the flux is positive. This problem is obviated by the first term on the right-hand side of (4.6), though clearly this places restrictions on the size of σ_{in}, which we shall investigate in more detail below. Lastly, the variance of $\sigma_{\mathrm{in}}(t)$ makes the general problem more complicated than that of a standard Stefan problem.

To obtain the operator that holds in the rubber, we substitute (3.19) and (3.20) in (2.9a) to obtain

$$\frac{\partial C_0^{\mathrm{r}}}{\partial t}=(D_{\mathrm{r}}+bE_{\mathrm{r}})\frac{\partial^2 C_0^{\mathrm{r}}}{\partial x^2}. \tag{4.7}$$

Note that the equation is Fickian in nature, since the rubbery state of the polymer is much closer to a Fickian system than is the glass [14, p. 42]. However, the effects of the pseudo-stress are still felt *via* the bE_{r} term. The remaining conditions on C_0^{r} come from the leading order of (2.10) and (2.12a):

$$C_0^{\mathrm{r}}(x,0)=1,\quad C_0^{\mathrm{r}}(s(t),t)=C_*. \tag{4.8}$$

We simplify our work by specializing to the case of constant $\sigma_{\text{in}}(t)$ in (4.6). Then (4.6–4.8) may be solved by using a standard similarity-variable approach in the variable $x/\sqrt{t}$. Thus the front must move like $t^{1/2}$; for later algebraic simplicity we take

$$s(t) = 2s_0\sqrt{(D_{\text{r}} + bE_{\text{r}})t}. \tag{4.9}$$

Since no coupling terms appear in (4.7) and (4.8), we may solve for the solution in the rubber first, then use (4.6) to solve for the interface position. Due to the simple form of the boundary conditions, all solutions are then written in terms of error functions. In particular, solving (4.7) subject to (4.8), we have that

$$C_0^{\text{r}}(x,t) = 1 + \frac{C_* - 1}{\operatorname{erfc}\ s_0}\operatorname{erfc}\ \left(\frac{x}{2\sqrt{(D_{\text{r}} + bE_{\text{r}})t}}\right). \tag{4.10}$$

4.2. The front position

The last piece of information needed is s_0, which can be obtained by substituting (4.10) in (4.6):

$$(D_{\text{r}} + bE_{\text{r}})\left[\frac{1}{\sqrt{\pi}}\left(\frac{1 - C_*}{\operatorname{erfc}\ s_0}\right)\exp\left(-s_0^2\right) + s_0 C_*\right] + \frac{\sigma_{\text{in}}}{2s_0} = \frac{D_{\text{g}}(C_* - C_{\text{ext}}) + bC_*}{2s_0}. \tag{4.11}$$

It can be shown that in order for there to be exactly one positive root s_0, the following condition must be satisfied:

$$\sigma_{\text{in}} < D_{\text{g}}(C_* - C_{\text{ext}}) + bC_*. \tag{4.12}$$

This condition on the surface pseudostress is quite similar to conditions imposed on the surface concentration to model the *self-regulation* of a polymer network [27, 33, 48, 49].

Figure 5 shows a graph of the left- and right-hand sides of (4.11). Here all parameters which did not vary were given the values in (3.9) and (3.12), and we have used the values

$$D_{\text{r}} = 2, \quad E_{\text{r}} = 3. \tag{4.13}$$

The intersection point of the left-hand side and right-hand side curves corresponds to the value of s_0 for the front. As D_{g} increases, from (2.12c) we note that the flux through the front increases. Since penetrant is being conveyed more quickly to the exposed surface, the front speed increases. On the other hand, as σ_{in} increases, from (4.2) we see that $\partial\sigma_0^{\text{g}}/\partial x$ decreases in order to reach the same value of σ at the front. Thus the flux through the front and hence its speed decreases.

To examine the variation of s_0 with C_* and C_{ext}, we rewrite (4.11) as

$$(D_{\text{r}} + bE_{\text{r}})\left[\frac{1}{\sqrt{\pi}}\left(\frac{1 - C_*}{\operatorname{erfc}\ s_0}\right)\exp\left(-s_0^2\right) + s_0 C_*\right] - \frac{C_*(b + D_{\text{g}})}{2s_0} = -\frac{D_{\text{g}}C_{\text{ext}} + \sigma_{\text{in}}}{2s_0}. \tag{4.14}$$

Figure 6 shows a graph of the left- and right-hand sides of (4.14). Again the intersection point is the value of s_0 determining the front. As C_* increases, the front speed increases. This is because not as much solvent needs to desorb, and hence the front moves faster. From (4.2) we see that C_{ext} plays a role in the glassy flux calculation similar to that of σ_{in}. Therefore, as C_{ext} increases, the front speed decreases.

The dependence of the front speed on the other three parameters (D_{r}, E_{r}, and b) is more subtle, since s depends on them not only through s_0, but also through (4.9). Thus, for these parameters, we simply plot the dependence of the front speed on them in Figure 7. Note that

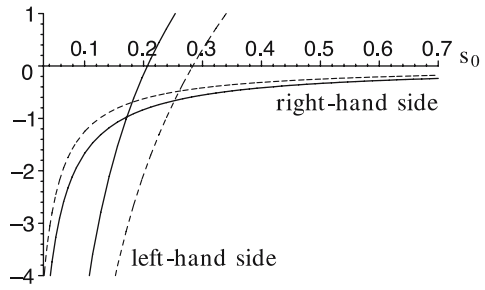

Figure 6. Plot of the expressions in (4.14). Solid lines: $C_* = 1/2$, $C_{\text{ext}} = 1/4$. Dotted lines: $C_* = 2/3$, $C_{\text{ext}} = 1/3$.

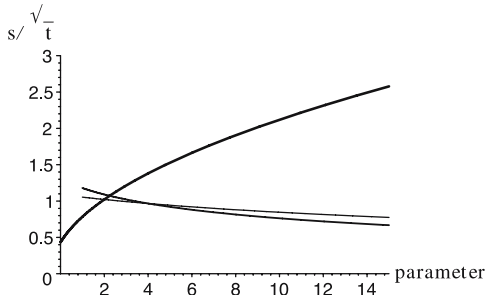

Figure 7. Plot of $s/\sqrt{t}$ vs. parameters in (4.9). In increasing order of thickness: D_r, E_r, b.

because of our choice of D_g in (3.9a), the graph for D_r starts at 1, since $D_r > D_g$. Similarly, our graph for E_r must start at 1.

As D_r and E_r increase, the front speed decreases. From Figure 5 we see that the bracketed quantity on the left-hand side of (4.11) is an increasing function of s_0. Thus, to balance the same glassy flux, an increase in either D_r or E_r causes a reduction in s_0. This reduction in s_0 is large enough to overwhelm the square-root dependence in (4.9). On the other hand, as b increases, the front speed increases. This is because increasing b also increases the glassy flux, which keeps the bracketed quantity from decreasing, which keeps s_0 increasing.

4.3. Solution profiles

Now that we have all necessary expressions for the functions, we can construct plots of our solution profiles. Given the previously listed parameters, we obtain

$$s_0 \approx 0{\cdot}1807. \tag{4.15}$$

Figure 8 shows a graph of the concentration vs. x for the times listed. Note the desorption overshoot in the glass as the concentration dips below the surface concentration before rising to C_* in a small layer near the front.

Figure 9 shows a graph of the σ vs. x for the times listed. Note the increasing pseudostress in the glassy region. These sorts of internal extrema, which are related to the buildup of stress associated with the glass-rubber change of state, have been seen in viscoelastic models of desorption [45, 46] and sorption [44] problems, as well as experimentally [47]. The flux contribution from σ in this region overwhelms the contribution from the concentration, thus forming an overall negative flux which continues the desorption of the polymer. The large negative gradient to the pseudostress in the layer near the front balances the large positive gradient in the concentration, as shown in (3.14), leading to an $O(1)$ total flux.

5. Conclusions

When saturated polymers near the glass-rubber transition temperature are desorbed, a glassy region will often form near the exposed surface. The formation of this skin cannot be described by Fick's Law alone. Due to the disparate length scales in the polymer network, it is reasonable to include nonlocal spatial dependence to model the nonstandard effects. Following [32], we assume that the chemical potential depends not only on the concentration $\tilde{C}$, but also on the pseudostress $\tilde{\sigma}$, which incorporates the nonlocal spatial dependence. Such

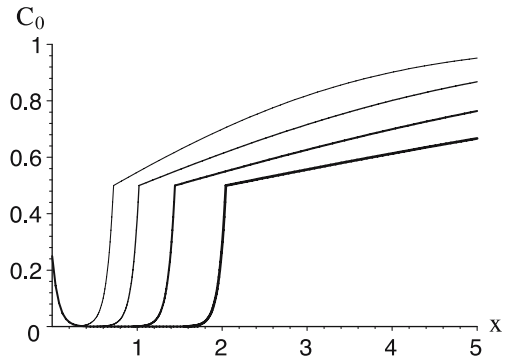

Figure 8. Plot of concentration vs. x. In increasing order of thickness: $t = 0{\cdot}5$, 1, 2, 4.

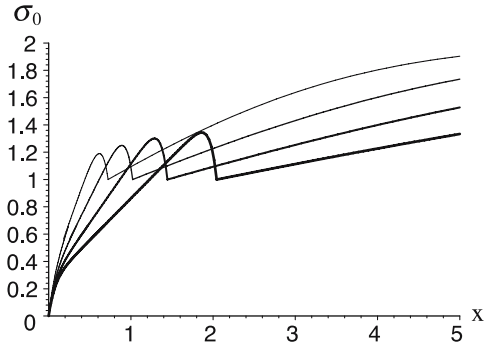

Figure 9. Plot of σ vs. x. In increasing order of thickness: $t = 0{\cdot}5$, 1, 2, 4.

an assumption results in a single partial integrodifferential equation which can be split into a set of two coupled partial differential equations.

Though these equations can be solved numerically, often it is the dependence of solutions on material parameters that is critical to understanding the underlying physics. Thus analytical solutions are needed, which necessitate the use of asymptotics and perturbation methods.

In order to solve the system analytically, we choose piecewise-constant forms for our nonlinear parameters β, D, and E. The resulting MBVP has the standard diffusion operator in the rubber, reflecting the fact that without a crystalline glassy structure, a polymer solution has behavior closely approximating a Fickian substance. Nevertheless, the effect of the polymer structure is seen in the effective diffusion coefficient, which includes both D_r and E_r.

In the glass, σ obeys a steady-state diffusion operator, and the concentration is zero to leading order. Thus, our model exhibits the phenomena of skinning, behavior also seen in viscoelastic models for polymer-penetrant systems [4, 5, 18, 19, 45, 46]. Since $C^g = 0$ is less than the interface values, the solution also exhibits desorption overshoot, as described in [33]. Thus to match the conditions at the exposed and glass-rubber interfaces, we insert boundary and interior layers in the concentration, each of which obeys the same nonlinear ODE. Because of the relationship between σ and C, we also need layers for the pseudostress. The solutions for σ exhibit maxima for x near but less than $s(t)$, which is consistent with a buildup in stress as the polymer changes states [44–47].

At $x = s(t)$, a Stefan-like condition was derived to couple the two operators. Though the presence of s in the denominator in one of the terms is unusual, it has been seen previously in viscoelastic MBVP models of these systems [26]. In addition, with the physically reasonable assumption of a constant imposed pseudostress, a similarity-variable approach can be used, and the front moves in a purely Fickian way. A condition on σ at the exposed interface is necessary to assure a solution; this condition is quite similar to the self-regulation found in other models of these systems [27, 33].

Though viscoelastic models have been used for years to describe non-Fickian diffusion phenomena, such models ignore the disparate length scales in a polymer-penetrant system. Though this oversight may be troubling from a theoretical perspective, the key question experimentally is whether ignoring spatial nonlocalities causes deficiencies in the model.

At the very least, by carefully validating our results by comparing them to experiments and the results of other models, we gain confidence that spatial nonlocalities have a role to play in certain polymer-penetrant systems. These agreements have been seen in both sorption

and desorption contexts. Whether this role is supplementary, complementary, or necessary will be determined only upon future examinations of polymer-penetrant systems.

Appendix A: Remarks on an initial layer

Note from Figure 8 that if we continue our solutions back towards $t=0$, the moving front is going to impinge upon the stationary boundary layer solution C_0^{b}. Since C_0^{b} is fixed in t, there must be an initial layer where the two layer solutions coalesce. As can be expected in such a singular perturbation problem, the layer equations become quite complicated, and so they would need to be solved numerically. Therefore, in this section we simply present the equations and discuss how their solutions would smoothly transition into the solutions previously derived.

To construct this layer at the corner of the x–t plane, we let

$$C^{\mathrm{g}}(x,t;\epsilon)=C_0^{\mathrm{i}}(\xi,\tau)+O(\epsilon^{1/2}),\quad \sigma^{\mathrm{g}}(x,t;\epsilon)=\sigma_0^{\mathrm{i}}(\xi,\tau)+O(\epsilon^{1/2}), \tag{A1a}$$

$$\xi=\frac{x}{\epsilon^{\frac{1}{2}}},\quad \tau=\frac{t}{\epsilon}. \tag{A1b}$$

These scalings imply that $\xi/\sqrt{\tau}=x/\sqrt{t}$, so our new variables obey the original similarity-variable law.

Substituting (A1) in (2.11a) and (2.8b), the leading order is again given by the operators in (3.6b) and (3.8a). Substituting (A1) in the conservation of mass equation yields the same operator as in (2.8a) because our new variables obey the similarity-variable law. Thus by combining the operators in (3.8a) and (2.8a), we have the following evolution equation for C^{i}:

$$\frac{\partial C_0^{\mathrm{i}}}{\partial\tau}=D_{\mathrm{g}}\frac{\partial^2 C_0^{\mathrm{i}}}{\partial\xi^2}-bC_0^{\mathrm{i}}+\left(\frac{\partial C_0^{\mathrm{i}}}{\partial\xi}\right)^2, \tag{A2}$$

which is not solvable in closed form.

The initial layer in the glass implies an initial layer in the rubber. Thus we assume the following forms:

$$C^{\mathrm{r}}(x,t;\epsilon)=C_0^{+}(\xi,\tau)+O(\epsilon^{1/2}),\quad \sigma^{\mathrm{r}}(x,t;\epsilon)=\sigma_0^{+}(\xi,\tau)s+O(\epsilon^{1/2}). \tag{A3}$$

Substituting (A3) in the conservation of mass equation, we obtain the same operator as in (2.9a) because of the similarity-variable law. The leading order of (2.9b) becomes

$$\sigma_0^{+}=bC_0^{+}-\left(\frac{\partial C_0^{+}}{\partial\xi}\right)^2,$$

which, when combined with the operator in (2.9a), yields

$$\frac{\partial C_0^{+}}{\partial\tau}=(D_{\mathrm{r}}+bE_{\mathrm{r}})\frac{\partial^2 C_0^{+}}{\partial\xi^2}-E_{\mathrm{r}}\frac{\partial}{\partial\xi^2}\left(\frac{\partial C_0^{+}}{\partial\xi}\right)^2, \tag{A4}$$

which is also not solvable in closed form.

Nevertheless, we may make the following remarks to indicate how Equations (A2) and (A4) resolve any problems we might encounter when taking our outer solutions as $t\to 0$:

A.1. Polymer must initially be rubbery

With the boundary condition for C^{i} being given by (3.6b), we note that $C_0^{\mathrm{i}}(0,\tau) \neq C_{\mathrm{ext}}$ for all τ. Instead, it evolves over time, finally reaching C_{ext} as $\tau \to \infty$, where the steady state of the governing operator (2.8a) implies that the flux becomes zero. Since the concentration at the boundary changes with time, we may now track the evolution of the surface concentration from its initial value of 1. Thus for some $\tau < \tau_*$, the polymer is *completely* in the rubber. This contrasts with our original formulation, where $s(0) = 0$ and the interface is immediately glassy. In the interval $0 \leq \tau \leq \tau_*$, the radiation condition is given by substituting (A3) into (2.11a), which also leads to the operator in (3.6b). Because of this form, we see that the flux through the interface is $O(\epsilon^{-1/2})$ when the polymer is rubbery. This comports with experimental results indicating that desorption is faster in the rubber than in the glass [38, 42, 43].

A.2. Front progression in initial layer

If we denote the front position in the initial layer as $\xi = s_\xi(\tau)$, then $s_\xi(\tau_*) = 0$. Since the scaling for ξ is the same as the scaling for ζ in (3.13a), we see that $\zeta = \xi - s_\xi$, and hence is no longer a layer. Thus $s_\xi = O(1)$ and one can track the front's progression through the corner layer directly without inserting another internal layer.

A.3. Replication of previous boundary and internal layers

As $\tau \to \infty$, for finite ξ equation (A2) reduces to (3.8b). Thus there is a smooth transition to the boundary-layer solution C_0^{b} about $\xi = 0$ and to the interior-layer solution C^- about $\xi = s_\xi(\tau)$ [since both obey the operator in (3.8b)].

A.4. Replication of previous rubbery solution

As ξ and τ get large in such a way that $\xi/\sqrt{\tau} = x/\sqrt{t}$ remains constant, (A4) reduces to (4.7) on the (x,t) scale. Thus our initial-layer solution matches our previous rubbery solution.

Acknowledgments

I wish to thank the reviewers for many helpful suggestions. This work was performed under National Science Foundation grant DMS-9407531. Many of the calculations herein were checked with the assistance of Maple. Portions of this manuscript were produced during a sabbatical stay at the University of Maryland, Baltimore County.

References

1. N. Thomas and A.H. Windle, Transport of methanol in poly-(methyl-methocry-late). *Polymer* 19 (1978) 255–265.
2. M. Vinjamur and R.A. Cairncross, A high airflow drying experimental set-up to study drying behavior of polymer solvent systems. *Drying Tech. J.* 19 (2001) 1591–1612.
3. M. Vinjamur and R.A. Cairncross, Experimental investigations of trapping skinning. *J. Appl. Polym. Sci.* 83 (2002) 2269–2273.
4. M. Vinjamur and R.A. Cairncross, A non-Fickian non-isothermal model for drying of polymer coatings. *AIChE J.* 48 (2002) 2444–2458.
5. R.A. Cairncross and C.J. Durning, A model for drying of viscoelastic coatings. *AIChE J.* 42 (1996) 2415–2425.
6. R.A. Cairncross, L.F. Francis and L.E. Scriven, Competing drying and reaction mechanisms in the formation of sol-to-gel films, fibers, and spheres. *Drying Tech. J.* 10 (1992) 893–923.

7. R.A. Cairncross, L.F. Francis and L.E. Scriven, Predicting drying in coatings that react and gel: drying regime maps. *AIChE J*. 42 (1996) 55–67.
8. E. Ben-Yoseph and R.W. Hertel, Computer modeling of sugar crystallization during drying of thin sugar films. *J. Crys. Growth* 198/199 (1999) 1294–1298.
9. E. Ben-Yoseph, R.W. Hertel and D. Howling, Three dimensional model of phase transition of thin sucrose films during drying. *J. Food Engng*. 44 (2000) 13–22.
10. S. Simal, A. Femenia, P. Llull and C. Rossello, Dehydration of aloe vera: Simulation of drying curves and evaluation of functional properties. *J. Food Engng*. 43 (2000) 109–114.
11. J. Crank, The influence of concentration-dependent diffusion on rate of evaporation. *Proc. Phys. Soc*. 63 (1950) 484–491.
12. J. Crank, Diffusion in media with variable properties, part III: diffusion coefficients which vary discontinuously with concentration. *Trans. Faraday Soc*. 47 (1951) 450–461.
13. C.A. Finch (ed.), *Chemistry and Technology of Water-Soluble Polymers*. New York: Plenum (1983) 380 pp.
14. W.R. Vieth, *Diffusion in and Through Polymers: Principles and Applications*. Oxford: Oxford University Press (1991) 322 pp.
15. J.S. Vrentas, C.M. Jorzelski and J.L. Duda, A Deborah number for diffusion in polymer-solvent systems. *AIChE J*. 21 (1975) 894–901.
16. M.O. Ngui and S.K. Mallapragada, Understanding isothermal semicrystalline polymer drying: mathematical models and experimental characterization. *J. Polym. Sci B* 36 (1998) 2771–2780.
17. G.W. Powers and J.R. Collier, Experimental modelling of solvent-casting thin polymer films. *Polym. Engng. Sci*. 30 (1990) 118–23.
18. D.A. Edwards, A mathematical model for trapping skinning in polymers. *Stud. Appl. Math.* 99 (1997) 49–80.
19. D.A. Edwards, Trapping skinning in polymers: theoretical predictions. *Chem. Engng. Commun.* 166 (1998) 201–216.
20. M. Dabral, Solidification of coatings: theory and modeling of drying, curing, and microstructure growth. Ph.D. thesis, University of Minnesota (1999) 333 pp.
21. M.O. Ngui and S.K. Mallapragada, Quantitative analysis of crystallization and skin formation during isothermal solvent removal from semicrystalline polymers. *Polymer* 40 (1999) 5393–5400.
22. I.H. Romdhane, P.E. Price, Jr., C.A. Miller, P.T. Benson and S. Wang, Drying of glassy polymer films. *Ind. Engng. Chem. Res*. 40 (2001) 3065–3075.
23. H.L. Frisch, Sorption and transport in glassy polymers—a review. *Polym. Engng. Sci*. 20 (1980) 2–13.
24. C.J. Durning and M. Tabor, Mutual diffusion in concentrated polymer solutions under a small driving force. *Macromolecules* 19 (1986) 2220–2232.
25. C.J. Durning, D.A. Edwards and D.S. Cohen, Perturbation analysis of Thomas' and Windle's model of case II transport. *AIChE J*. 42 (1996) 2025–2035.
26. D.A. Edwards and D.S. Cohen, An unusual moving boundary condition arising in anomalous diffusion problems. *SIAM J. Appl. Math*. 55 (1995) 662–676.
27. D.A. Edwards and D.S. Cohen, A mathematical model of a dissolving polymer. *AIChE J*. 41 (1995) 2345–2355.
28. L.H. Sperling, *Introduction to Physical Polymer Science*, 3rd ed. New York: John Wiley and Sons (2001) 671 pp.
29. H. Fujita, Organic vapors above the glass transition temperature. In: J. Crank and G.S. Park (eds.), *Diffusion in Polymers*, New York: Academic Press (1996) pp. 75–105.
30. M. Doi and S.F. Edwards, *The Theory of Polymer Dynamics*. Oxford: Clarendon Press (1986) 391 pp.
31. H.C. Öttinger, *Stochastic Processes in Polymeric Fluids: Tools and Examples for Developing Simulation Algorithms*. New York: Springer-Verlag (1996) 362 pp.
32. D.A. Edwards, A spatially nonlocal model for polymer-penetrant diffusion. *J. Appl. Math. Phys*. 52 (2001) 254–288.
33. D.A. Edwards and R.A. Cairncross, Desorption overshoot in polymer-penetrant systems: Asymptotic and computational results. *SIAM J. Appl. Math.* 63 (2002) 98–115.
34. D.S. Cohen, Theoretical models for diffusion in glassy polymers. *J. Polym. Sci. B* 21 (1983) 2057–2065.
35. D.S. Cohen, Theoretical models for diffusion in glassy polymers. II. *J. Polym. Sci. B* 22 (1984) 1001–1009.
36. J. Crank, A theoretical investigation of the influence of molecular relaxation and internal stress on diffusion in polymers. *J. Polym. Sci.* 11 (1953) 151–168.
37. C.Y. Hui, K.C. Wu, R.C. Lasky and E.J. Kramer, Case II diffusion in polymers. II. Steady state front motion. *J. Appl. Phys*. 61 (1987) 5137–5149.

38. S. Joshi and G. Astarita, Mathematical model of the desorption of swelling solvents from swollen polymer films. *Polymer* 20 (1979) 1217–1220.
39. T. Qian and P.L. Taylor, From the Thomas-Windle model to a phenomenological description of Case-II diffusion in polymers. *Polymer* 41 (2000) 7159–7163.
40. G. Rossi, P.A. Pincus and P.G. de Gennes, A phenomenological description of Case II diffusion in polymeric materials. *Europhys. Letts*. 32 (1995) 391–396.
41. J.H. Petroupoulos and P.P. Roussis, The influence of transverse differential swelling stresses on the kinetics of sorption of penetrants by polymer materials. *J. Membr. Sci*. 3 (1978) 343–356.
42. E. Bagley and F.A. Long, 2-Stage sorption and desorption of organic vapors in cellulose acetate. *J. Am. Chem. Soc*. 77 (1955) 2172–2178.
43. M.A. Hoyt and C.M. Balik, Diffusivity of a drug preservative in bromobutyl rubber. *Polym. Engng. Sci*. 36 (1996) 1862–1868.
44. D.A. Edwards, Constant front speed in weakly diffusive non-Fickian systems. *SIAM J. Appl. Math*. 55 (1995) 1039–1058.
45. D.A. Edwards, An asymptotic analysis of polymer desorption and skinning. *Macromol. Theory Sim*. 8 (1999) 10–14.
46. D.A. Edwards, Skinning during desorption of polymers: an asymptotic analysis. *SIAM J. Appl. Math.* 59 (1999) 1134–1155.
47. J.C. Phillips, Stress relaxation of elongated strips of poly(vinylidene fluoride) in ethyl acetate vapor. *Polym. Engng. Sci*. 37 (1997) 291–307.
48. J. Crank and G.S. Park, Diffusion in high polymers: Some anomalies and their significance. *Trans. Faraday Soc.* 47 (1951) 1072–1084.
49. F.A. Long and D. Richman, Concentration gradients for diffusion of vapors in glassy polymers and their relation to time dependent diffusion phenomena. *J. Am. Chem. Soc.* 82 (1960) 513–519.